IV International Conference on Computational Methods for Coupled Problems in Science and Engineering
COUPLED PROBLEMS 2011
M. Papadrakakis, E. Oñate and B. Schrefler (Eds)

COMPARATIVE PATIENT-SPECIFIC FSI MODELING OF CEREBRAL ANEURYSMS

KENJI TAKIZAWA*, TYLER BRUMMER†, TAYFUN E. TEZDUYAR† AND PENG R. CHEN‡

*Department of Modern Mechanical Engineering and
Waseda Institute for Advanced Study, Waseda University
1-6-1 Nishi-waseda, Shinjuku-ku,Tokyo 169-8050, JAPAN

†Mechanical Engineering, Rice University – MS 321
6100 Main Street, Houston, TX 77005, USA

‡Cerebrovascular and Neuro-Endovascular Program
Skull Base Program, Department of Neurosurgery
Mischer Neuroscience Institute
University of Texas Medical School at Houston
6400 Fannin, Houston, TX 77030, USA

Key words: Cardiovascular fluid mechanics, Cerebral aneurysms, Patient-specific modeling, Fluid–structure interaction, Space–time techniques

Abstract. We consider a total of ten cases, at three different locations, half of which ruptured sometime after the images were taken. We use the stabilized space–time FSI technique developed by the Team for Advanced Flow Simulation and Modeling, together with a number of special techniques targeting arterial FSI modeling. We compare the ten cases based on the wall shear stress, oscillatory shear index, and the arterial-wall stress. We also investigate how simpler approaches to computer modeling of cerebral aneurysms perform compared to FSI modeling.

1 INTRODUCTION

Arterial fluid mechanics modeling is now a significant part of computational biomechanics research. Much of this has been in patient-specific modeling of cerebral arteries with aneurysm, taking into account the fluid–structure interaction (FSI) between the blood flow and arterial walls. This class of research has been benefiting much from computational mechanics techniques targeting FSI modeling in general. The Deforming-Spatial-Domain/Stabilized Space–Time (DSD/SST) formulation [1, 2] was developed by the Team for Advanced Flow Simulation and Modeling (T★AFSM) for flow computations with moving boundaries and interfaces, including FSI. The formulation is based

on the Streamline-Upwind/Petrov-Galerkin (SUPG) [3] and Pressure-Stabilizing/Petrov-Galerkin (PSPG) [1] methods. The DSD/SST formulation is used with the mesh update methods [4] developed by the T★AFSM. New-generation DSD/SST formulations were introduced by the T★AFSM in [5]. The stabilized space–time FSI (SSTFSI) technique, which is based on the new-generation DSD/SST formulations, was also introduced in [5]. The SSTFSI technique, with special techniques developed by the T★AFSM for arterial FSI, has been extensively used for arterial modeling, with emphasis on cerebral aneurysms [6, 7]. The special techniques include methods for calculating an estimated zero-pressure (EZP) arterial geometry [8, 9], a special mapping technique for specifying the velocity profile at an inflow boundary with non-circular shape [10], techniques for using variable arterial wall thickness [10, 9], mesh generation techniques for building layers of refined fluid mechanics mesh near the arterial walls [11, 9], a recipe for pre-FSI computations that improve the convergence of the FSI computations [6, 8], and techniques [12] for the projection of fluid–structure interface stresses, calculation of the wall shear stress (WSS) and calculation of the oscillatory shear index (OSI).

In this paper, which is a short version of a recently-submitted journal article [7], we focus on comparative patient-specific FSI modeling of cerebral aneurysms. We have ten cases, at three different locations, half of which ruptured sometime after the images were taken. We compare these cases based on the WSS, OSI and the arterial-wall stress. We also investigate how simpler methods perform compared to FSI modeling.

2 COMPUTATIONAL TECHNIQUES AND GENERAL CONDITIONS

We use the SSTFSI technique [5], with special techniques for arterial FSI. The special techniques include a mapping technique for specifying the inflow velocity profile [10], methods [12] for the projection of fluid–structure interface stresses and calculation of the WSS and OSI, and the Separated Stress Projection (SSP) technique [13, 9]. Special boundary condition techniques [9] are used for inclined inflow and outflow planes. The fully-discretized, coupled fluid, structure and mesh-moving equations are solved with the quasi-direct coupling technique (see Section 5.2 in [5]). In iteratively solving the linear systems involved at every nonlinear iteration, we use "Selective Scaling" technique (see Remark 14 in [5]) to shift the emphasis between the fluid and structure parts. In some cases, we also use selective scaling to shift the emphasis between the parts of the fluid equations corresponding to the momentum conservation and incompressibility constraint [14].

The fluid and structure properties can be found in [9]. At the inflow we specify the velocity profile as a function of time, by using a special technique [9]. The Womersley parameter, which appears in that technique, is defined as $\Upsilon = r_{\mathrm{B}}\sqrt{2\pi/\nu T}$. Here r_{B} is the average radius of the inflow cross-sectional area, which comes from the image-based data, ν is the kinematic viscosity, and T is the period of the cardiac cycle, which is taken as 1 s. The volumetric flow rate (which is calculated based on a velocity waveform that represents the cross-sectional maximum velocity) is scaled by a factor. The scaling factor is determined in such a way that the scaled flow rate, when averaged over the cardiac

cycle, yields a target WSS for Poiseuille flow over an equivalent cross-sectional area. The target WSS is 10 dyn/cm^2 in the current T★AFSM computations. The time-step size is 3.333×10^{-3} s. The number of nonlinear iterations per time step is 6. The number of GMRES [15] iterations per nonlinear iteration for the fluid+structure block was chosen such that mass balance is satisfied to within at most 5% for each case. For all six nonlinear iterations the fluid scale is 1.0 and the structure scale is 100. In three of the cases, the fluid scales for the momentum conservation and incompressibility constraint are 1.0 and 10. For the mesh moving block the number of GMRES iterations is 30. All computations were completed without any remeshing. For additional description of the computational techniques used and general conditions, see [7].

3 CASE STUDIES

Ten cases are studied from three locations: 4 Middle Cerebral Artery (MCA), 4 Anterior Communicating Artery (Acom), and 2 Basilar Artery. Half of each location ruptured sometime after the images were taken. Figures 1–3 show the lumen geometries. The

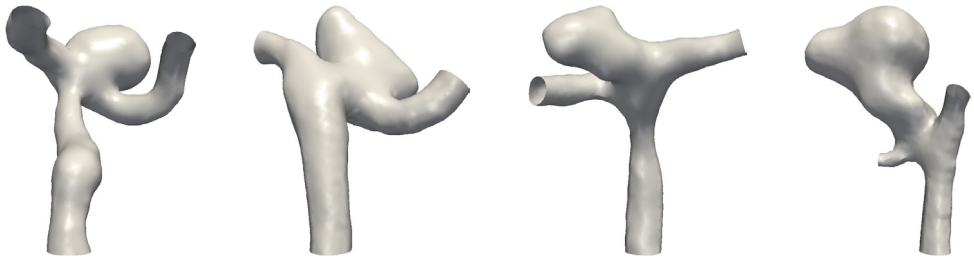

Figure 1: Arterial lumen geometry obtained from voxel data for the MCA models.

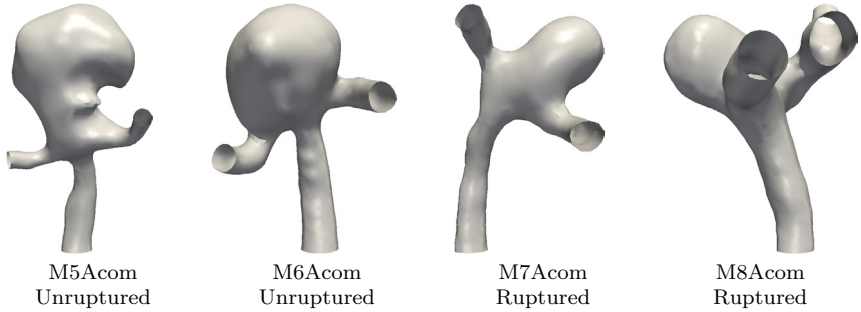

Figure 2: Arterial lumen geometry obtained from voxel data for the Acom models.

physical parameters are shown in Table 1. The number of nodes vary between 8,000 and 18,000 for the structure (hexahedral) meshes and between 33,000 and 60,000 for the fluid (tetrahedral) meshes. For all models the maximum WSS occur at the maximum inflow

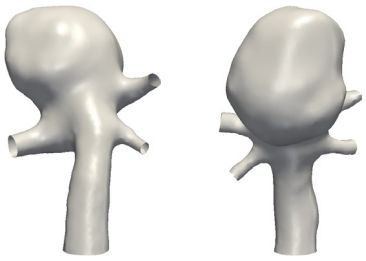

M9Basilar Unruptured M10Basilar Ruptured

Figure 3: Arterial lumen geometry obtained from voxel data for the Basilar models.

Model	D_{I}	D_{O1}	D_{O2}	D_{O3}	Υ	$Q_{\max}$
M1MCA	2.43	2.42	1.87		1.52	0.51
M2MCA	1.56	1.41	1.38		0.97	0.12
M3MCA	2.50	1.49	1.43		1.57	0.56
M4MCA	1.70	1.21	0.81		1.06	0.08
M5Acom	3.05	1.78	1.75		1.91	1.08
M6Acom	3.13	2.12	2.12		1.96	1.20
M7Acom	1.02	0.90	0.80		0.64	0.04
M8Acom	1.94	2.31	2.17	1.38	1.21	0.25
M9Basilar	2.60	1.31	1.01	0.88	1.63	0.64
M10Basilar	3.03	1.34	1.04	1.01	1.90	1.06

Table 1: Physical parameters. Diameters are in mm and peak volumeteric flow rate is in ml/s. M10Basilar has a fourth outflow with diameter 0.93 mm.

flow rate of the cardiac cycle. Maximum and average WSS values are shown in Figure 4. Figures 5–9 show the OSI for all the models. The maximum structural stress in space and time occurs at the peak pressure. Figure 10 shows the maximum stress and maximum variation in stress for all the models. As a point of reference, we note from [16] that the breaking strength of saccular aneurysms is in the range of 730–1,900 kPa.

4 NUMERICAL-PERFORMANCE STUDIES

We investigate how simpler approaches to modeling of our ten cases compare to FSI modeling. The three simpler modeling techniques are computing the blood flow with the artery shape held fixed at the average pressure (92 mm Hg), computing the arterial wall deformation with a prescribed, time-dependent pressure, and computing the blood flow with the prescribed arterial shape coming from that arterial-wall computation. We refer to these modeling techniques as "Rigid Artery (RA)", "Structure (S)", and "Prescribed Shape (PS)" in this paper. For the RA and PS computations we compare the WSS and OSI. For the Structure computations, we compare the arterial-wall stress.

Figure 11 shows the maximum and average WSS for the FSI, RA, and PS techniques. We see the maximum WSS being almost the same for the FSI and PS computations. The shape for the PS comes from a structural mechanics only computation where the viscous forces from the fluid are not accounted for. This gives the PS a slightly smaller shape than the FSI shape resulting in WSS that is on average 2.5% higher than FSI. For the

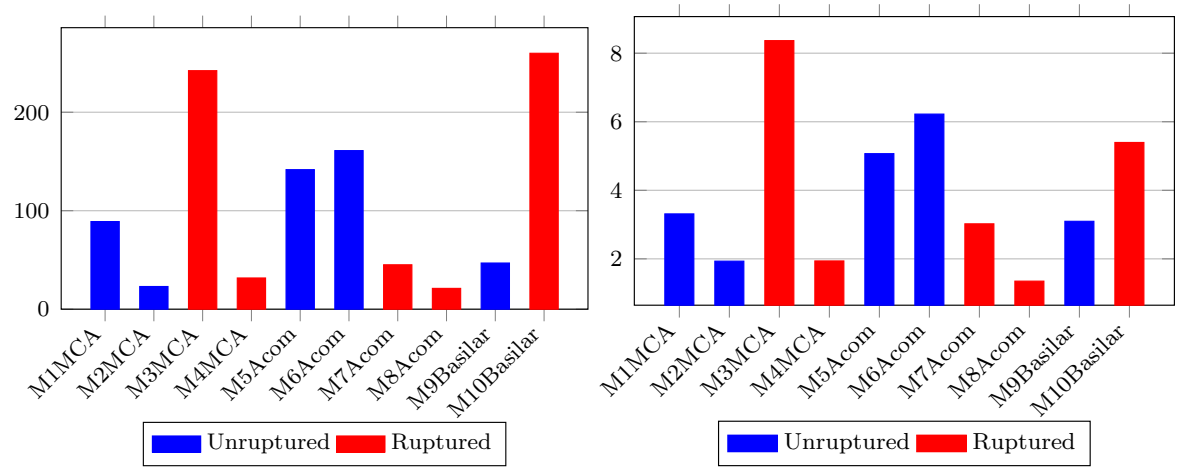

Figure 4: Maximum and average WSS (dyn/cm^2) in space and time.

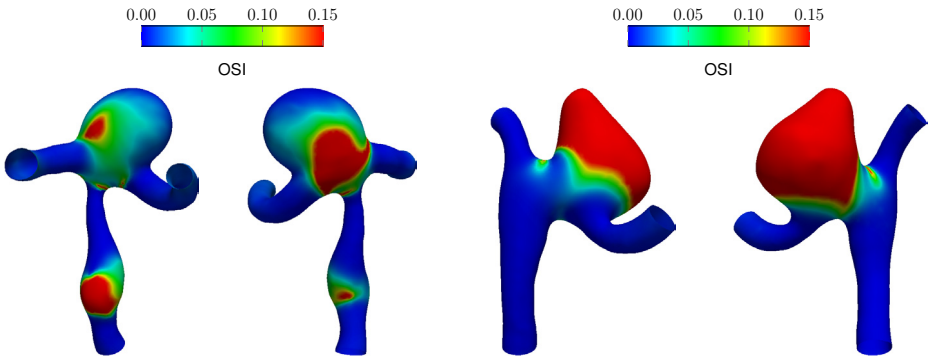

Figure 5: OSI for M1MCA and M2MCA.

RA computations, we see a clear pattern of higher WSS than the FSI. The RA shape is inflated to the average pressure, which, over the interval of peak inflow flow rate, is smaller than the FSI shape over that same interval. For this reason, we see the average WSS to be 4.2% higher than FSI. Using M5Acom as a sample model, we compare the spatial distribution of the OSI obtained with the PS and RA techniques (Figures 12 and 13) to those obtained with the FSI computation. The differences between the RA and FSI computations show the need for computing with a deformable structure. Figure 14 shows the maximum arterial-wall stress for the FSI and Structure techniques. The differences are less than 1%.

5 CONCLUDING REMARKS

We have presented an extensive comparative study based on patient-specific FSI modeling of cerebral aneurysms. We considered a total of ten artery models, coming from three different locations, half of which ruptured sometime after the images were taken.

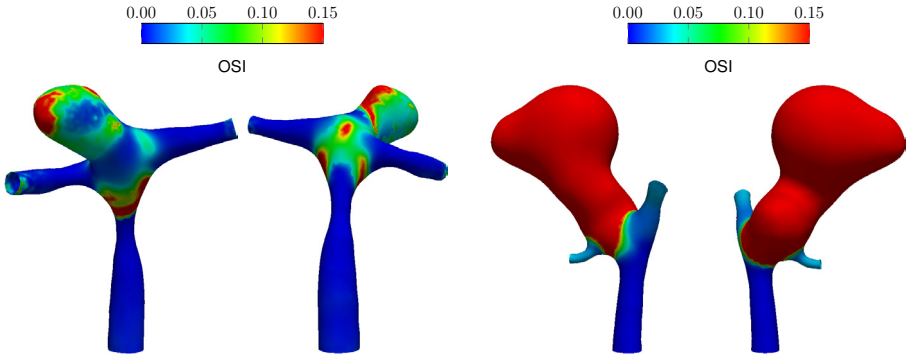

Figure 6: OSI for M3MCA and M4MCA.

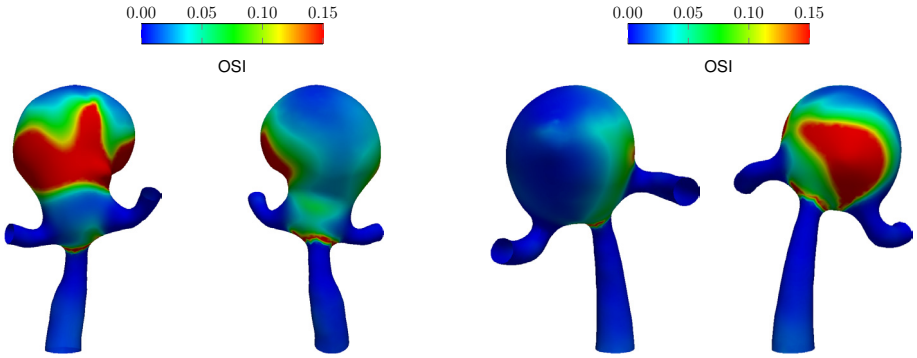

Figure 7: OSI for M5Acom and M6Acom.

We used the SSTFSI technique developed by the T★AFSM, together with a number of special techniques targeting arterial FSI modeling, which were also developed by the T★AFSM. We compared the WSS, OSI and the arterial-wall stress. We also showed how simpler approaches perform compared to FSI modeling. The simpler approaches were computing the blood flow with the artery shape held fixed, computing the arterial wall deformation with a prescribed, time-dependent pressure, and computing the blood flow with the prescribed arterial shape coming from that arterial wall computation.

ACKNOWLEDGMENT

This work was supported partly by John & Ann Doerr Fund for Computational Biomedicine. It was also supported partly by NSF Grant CNS-0821727. The 3DRA research at the Memorial Hermann was supported by the Weatherhead Foundation. We thank Dr. Ryo Torii for the velocity wave form.

REFERENCES

[1] T.E. Tezduyar, "Stabilized finite element formulations for incompressible flow computations", *Advances in Applied Mechanics*, **28** (1992) 1–44.

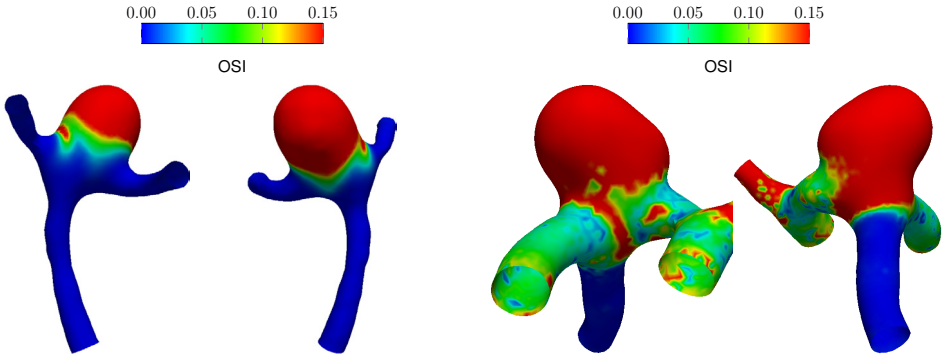

Figure 8: OSI for M7Acom and M8Acom.

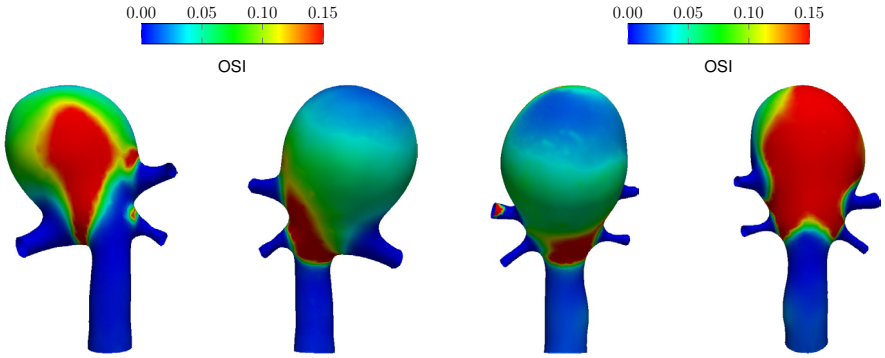

Figure 9: OSI for M9Basilar and M10Basilar.

[2] T.E. Tezduyar, "Computation of moving boundaries and interfaces and stabilization parameters", *International Journal for Numerical Methods in Fluids*, **43** (2003) 555–575.

[3] A.N. Brooks and T.J.R. Hughes, "Streamline upwind/Petrov-Galerkin formulations for convection dominated flows with particular emphasis on the incompressible Navier-Stokes equations", *Computer Methods in Applied Mechanics and Engineering*, **32** (1982) 199–259.

[4] T. Tezduyar, S. Aliabadi, M. Behr, A. Johnson, and S. Mittal, "Parallel finite-element computation of 3D flows", *Computer*, **26** (1993) 27–36.

[5] T.E. Tezduyar and S. Sathe, "Modeling of fluid–structure interactions with the space–time finite elements: Solution techniques", *International Journal for Numerical Methods in Fluids*, **54** (2007) 855–900.

[6] T.E. Tezduyar, S. Sathe, T. Cragin, B. Nanna, B.S. Conklin, J. Pausewang, and M. Schwaab, "Modeling of fluid–structure interactions with the space–time finite

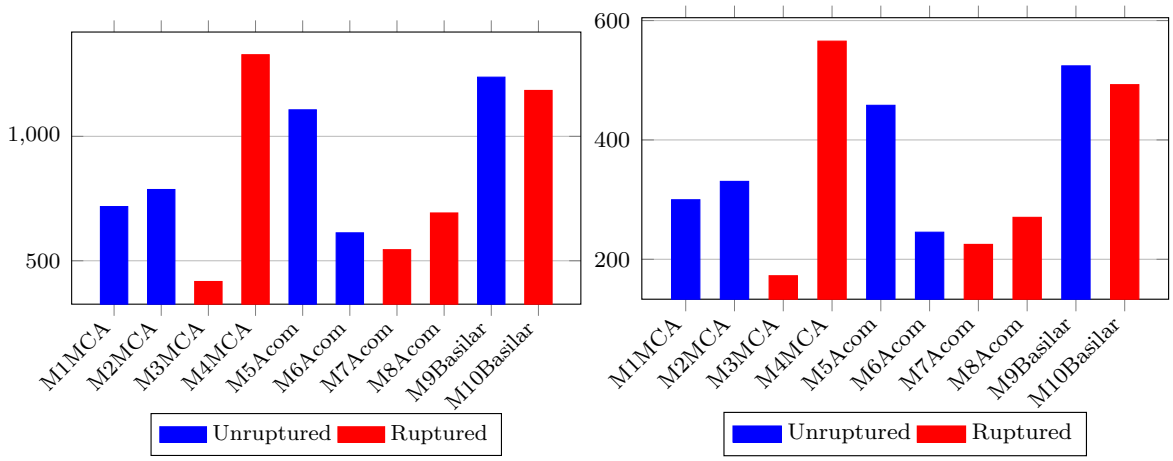

Figure 10: Maximum stress and maximum variation in stress (kPa) in space and time.

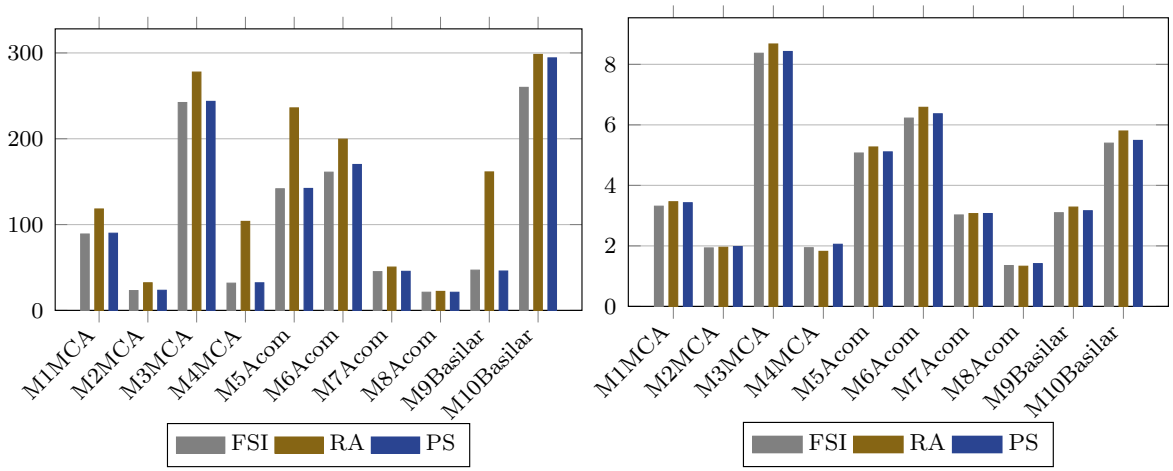

Figure 11: Maximum and average WSS (dyn/cm^2) in space and time.

elements: Arterial fluid mechanics", *International Journal for Numerical Methods in Fluids*, **54** (2007) 901–922.

[7] K. Takizawa, T. Brummer, T.E. Tezduyar, and P.R. Chen, "A comparative study based on patient-specific fluid–structure interaction modeling of cerebral aneurysms", *Journal of Applied Mechanics*, submitted, 2011.

[8] T.E. Tezduyar, S. Sathe, M. Schwaab, and B.S. Conklin, "Arterial fluid mechanics modeling with the stabilized space–time fluid–structure interaction technique", *International Journal for Numerical Methods in Fluids*, **57** (2008) 601–629.

[9] T.E. Tezduyar, K. Takizawa, T. Brummer, and P.R. Chen, "Space–time fluid–structure interaction modeling of patient-specific cerebral aneurysms", *International*

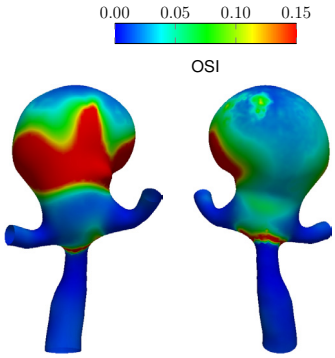

Figure 12: PS OSI for M5Acom.

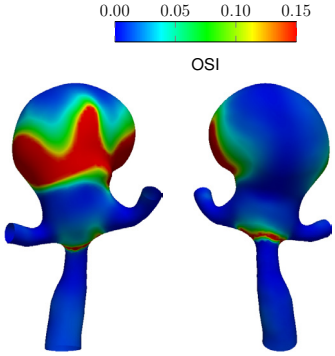

Figure 13: RA OSI for M5Acom.

Journal for Numerical Methods in Biomedical Engineering, published online, DOI: 10.1002/cnm.1433, February 2011.

[10] K. Takizawa, J. Christopher, T.E. Tezduyar, and S. Sathe, "Space–time finite element computation of arterial fluid–structure interactions with patient-specific data", *International Journal for Numerical Methods in Biomedical Engineering*, **26** (2010) 101–116.

[11] T.E. Tezduyar, M. Schwaab, and S. Sathe, "Sequentially-Coupled Arterial Fluid–Structure Interaction (SCAFSI) technique", *Computer Methods in Applied Mechanics and Engineering*, **198** (2009) 3524–3533.

[12] K. Takizawa, C. Moorman, S. Wright, J. Christopher, and T.E. Tezduyar, "Wall shear stress calculations in space–time finite element computation of arterial fluid–structure interactions", *Computational Mechanics*, **46** (2010) 31–41.

[13] T.E. Tezduyar, S. Sathe, J. Pausewang, M. Schwaab, J. Christopher, and J. Crabtree, "Interface projection techniques for fluid–structure interaction modeling with moving-mesh methods", *Computational Mechanics*, **43** (2008) 39–49.

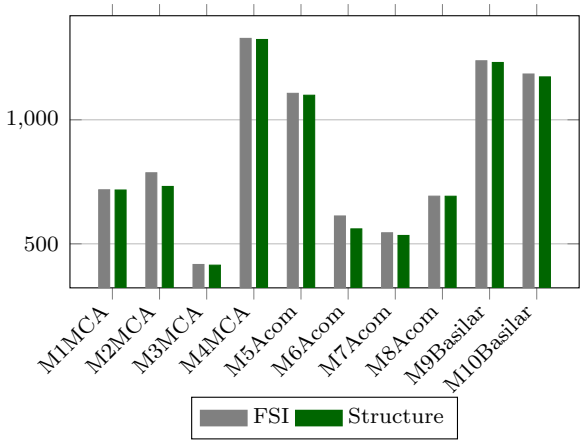

Figure 14: Maximum stress (kPa) in space and time.

[14] K. Takizawa, C. Moorman, S. Wright, J. Purdue, T. McPhail, P.R. Chen, J. Warren, and T.E. Tezduyar, "Patient-specific arterial fluid–structure interaction modeling of cerebral aneurysms", *International Journal for Numerical Methods in Fluids*, **65** (2011) 308–323.

[15] Y. Saad and M. Schultz, "GMRES: A generalized minimal residual algorithm for solving nonsymmetric linear systems", *SIAM Journal of Scientific and Statistical Computing*, **7** (1986) 856–869.

[16] D.J. Macdonald, H.M. Finlay, and P.B. Canham, "Directional wall strength in saccular brain aneurysms from polarized light microscopy", *Annals of Biomedical Engineering*, **28** (2000) 533–542.